Pramana – J. Phys. (2017) 89:55
DOI 10.1007/s12043-017-1450-8

Alternative search strategies to explore ATLAS diboson excess

CHARANJIT K KHOSA

Centre for High Energy Physics, Indian Institute of Science, Bengaluru 560 012, India
E-mail: khosacharanjit@chep.iisc.ernet.in

Published online 5 October 2017

Abstract. We consider the s-channel resonance to fit the 2 TeV ATLAS diboson excess. We address the production mechanism of the resonance, its decay and coupling measurement. In order to explain only the hadronic channel excess, we consider the scenario where resonance decays to two new beyond Standard Model (BSM) particles (in the mass range of W/Z boson) and also explore the possibility of three-particle BSM final state mimicking diboson excess. Techniques suggested in this work are generic and could be used for heavy BSM resonance searches.

Keywords. Resonance; beyond Standard Model; diboson.

PACS Nos **13.38.−b; 12.60.−i**

1. Introduction

ATLAS experiment has reported several excesses from Run-I (8 TeV) data. Diboson excess from the 2 TeV resonance decay is one of them [1]. The reported discrepancy is 3.4σ, 2.6σ and 2.9σ in WZ, WW and ZZ channels respectively. Although this excess has not been confirmed by the 13 TeV data [2], the analysis done in this context will be useful for the other heavy beyond Standard Model (BSM) resonance searches in the future. Any hint of new physics in the TeV energy range is exciting as most of the ultraviolet completions of Standard Model (SM) predict TeV scale particles. Several theoretical explanations have been given to explain this 2 TeV excess seen by the ATLAS experiment. Most popular among them are left–right symmetric models (where heavy resonance is identified as W'/Z') [3–5], composite Higgs model [6], heavy Higgs boson(s) [7–9], R-parity conserving [10] and violating [11] supersymmetric models, effective theory approach [12] etc.

The W/Z gauge bosons can also decay to semileptonic and leptonic final states, in addition to the hadronic final state but no significant excess has been seen in the semileptonic final states [13].

We have considered the s-channel resonance (R) and studied its production, decay and coupling measurement in detail. We estimate the expected number of events for leptonic and semileptonic processes. In order to explain only hadronic excess, we consider the two BSM particle final state. We also study the viability of three-particle final state mimicking diboson signal. We suggest new phenomenological signatures that one should look for while searching for the resonance.

2. Analysis

The decay product of the heavy resonance will be very boosted and their further decay products will be collimated to form a single fat jet (J). Two fat jet final state is considered to look for dibosons. ATLAS analysis uses C/A method with radius 1.2 for jet formation. They look for the pair of subjets inside the fat jet coming from the decay of W/Z bosons. The following final states could arise from the pair of gauge bosons

- JJ channel: Fully hadronic final state will have two fat jets. ATLAS experiment has observed excess in this channel. One can get this final state from WW, ZZ or WZ pairs. The following cuts are imposed to recognize the subjets inside the fat jet and to reduce the QCD background:
  - Fat jet pair invariant mass >1050 GeV, jet mass $m_J \in (82.4 \pm 13/92.8 \pm 13)$ GeV, pseudorapidity $|\eta| < 2$ and $(p_{\mathrm{T}}^{J_1} - p_{\mathrm{T}}^{J_2})/(p_{\mathrm{T}}^{J_1} + p_{\mathrm{T}}^{J_2}) < 0.15$ are used to tag W/Z bosons, where $p_{\mathrm{T}}^{J_1}$ and $p_{\mathrm{T}}^{J_2}$ are the p_{T} of the first and second jet respectively.
  - Number of charge tracks inside the fat jet should be less than 30 to remove the higher multiplicity gluons.

Table 1. Expected number of events for different leptonic channels at 13 TeV.

Channel	Cuts	No. of signal events (5 fb^{-1})			No. of background events (5 fb^{-1})
		WW	*ZZ*	*WZ*	
$l\nu J$	$p_{\mathrm{T}}^{l} > 25\,\mathrm{GeV},\ p_{\mathrm{T}}^{J} > 800\,\mathrm{GeV},\ p_{\mathrm{T}}^{l\nu} > 800\,\mathrm{GeV}$	65		30	20
llJ	$1.8\,\mathrm{TeV} < m_{llJ} < 2.2\,\mathrm{TeV},\ p_{\mathrm{T}}^{J} > 400\,\mathrm{GeV},\ p_{ll}^{\mathrm{T}} > 400\,\mathrm{GeV}$		30	10	2
$lll\nu$	$p_{\mathrm{T}}^{l_1} > 100\,\mathrm{GeV},\ p_{\mathrm{T}}^{l_2} > 100\,\mathrm{GeV},\ p_{\mathrm{T}}^{l_3} > 100\,\mathrm{GeV}$			4	4
$llll$	$p_{\mathrm{T}}^{l_1} > 60\,\mathrm{GeV},\ p_{\mathrm{T}}^{l_2} > 60\,\mathrm{GeV},\ p_{\mathrm{T}}^{l_3} > 60\,\mathrm{GeV},\ p_{\mathrm{T}}^{l_4} > 60\,\mathrm{GeV}$		1		2

– The cut on the rapidity difference $|y_1 - y_2| < 1.2$ is used to remove the large t-channel gluon-mediated background.

In addition to the above cuts, events with prompt electron and muon and $\not{E}_{\mathrm{T}} > 350\,\mathrm{GeV}$ are removed.

- $l\nu J$ channel: The 13 TeV analysis also includes this channel. There should be at least one W boson to get this final state. Therefore, either one could have WZ or WW from the resonance decay. In addition to the jet mass window ($65 < m_W < 105\,\mathrm{GeV}$, $70 < m_Z < 110\,\mathrm{GeV}$), other cuts used are $p_{\mathrm{T}}^{l} > 25\,\mathrm{GeV}$, $p_{\mathrm{T}}^{J} > 400\,\mathrm{GeV}$, $\not{E}_{\mathrm{T}} > 30\,\mathrm{GeV}$ and $p_{\mathrm{T}}(l\nu) > 400\,\mathrm{GeV}$ (vector sum of p_{T} vector of $\not{E}_{\mathrm{T}}$ and lepton). The main backgrounds for this channel are $W+$ jets, top quark pair production and non-resonant diboson production.
- llJ channel: This channel is sensitive to WZ and ZZ final states. Here an extra condition of same flavour opposite sign dilepton pair is demanded in addition to the previously discussed cuts. The invariant mass of lepton pair is required to be in the 65–115 GeV range. The main background processes are $Z+$ jets, top quark pair and non-resonant vector boson pair production.
- $lll\nu$ channel: For this channel, three isolated leptons, each with p_{T} and $\not{E}_{\mathrm{T}} > 25\,\mathrm{GeV}$ are required. Out of the three isolated leptons, two should have opposite-sign same-flavour and invariant mass of that pair of leptons should be close to m_Z mass as they are produced from the Z-decay. This channel is a probe of WZ final state.

Following the ATLAS strategy, we have calculated the number of events from all possible final states from the pair of gauge bosons that could be seen at 13 TeV [14]. We have used CalcHEP [15], PYTHIA [16] and fast jet [17] for parton level events, showering and jet formation respectively. The idea of considering all possible states is to distinguish WW, ZZ and WZ final states. The fully hadronic JJ final state can be obtained from any of the WW, ZZ and WZ pairs. But scenario in which one sees significant excess in the $l\nu J$ channel but no excess in the $lll\nu$ channel, corresponds to the WW final state. We have used track isolation to count the isolated leptons. We have considered the dominant backgrounds like $W+$jets, $Z+$jets and SM VV production. We assume $\sigma(pp \to R \to VV) \approx 100$ fb for all WW, ZZ and WZ final states. The optimized cuts used to increase the signal significance are given in table 1. We also estimate the 13 TeV signal to background ratio for the fully hadronic channel. We find that there will be 12 signal events corresponding to 32 background events with the 400 GeV p_{T} cut on fat jet but for an accurate background estimation, systematic uncertainty has to be considered properly. We can see from table 1 that WW channel could be distinguished with 5 fb^{-1} of data and fully leptonic channel could be probed at higher luminosity.

3. Two-particle final state

In order to explain the absence of leptonic and semileptonic final states, we consider the scenario where hadronic final state excess could be due to two BSM particles (X) having mass close to gauge bosons. The dominant decay modes of these particles are light quarks or gluons. Therefore, one will not see any excess in the semileptonic and leptonic final states. The Feynman diagram for this process is given in figure 1. We have simulated this final state using PYTHIA 6.4.28, tune (AUET-2B) and pdf-CTEQ6L1. In figure 2 we provide the number of charge tracks inside the highest p_{T} fat jet. We consider $u\bar{u}$, $c\bar{c}$, $b\bar{b}$ and gg final states. One can see that it is possible to distinguish gluon final state. The $b\bar{b}$ final state could be distinguished using b-tagging (efficiency will be <50% for the high p_{T} jets). The cut on the number of charge tracks will further reduce the signal selection efficiency for gluon final state. Therefore, one really needs large cross-section to get sufficient number of events.

The particle X could also decay to $\tau^+\tau^-$, but this branching fraction cannot be large because no BSM signal has been reported for the semileptonic channel. In

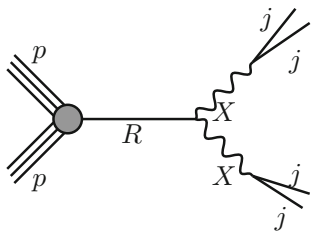

Figure 1. Feynman diagram for resonance decaying to a pair of the particle X.

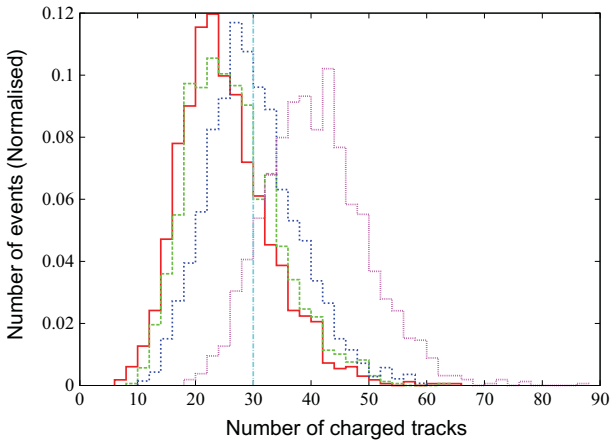

Figure 2. Normalized charge multiplicity distribution for the highest p_T jet formed by different ($u\bar{u}$ – red, $c\bar{c}$ – green, $b\bar{b}$ – blue and gg – violet) decay modes of the particle X.

some models, one could get two different BSM particles X and Y from R decay. Also, the spin of the particle X in these kinds of models can be observed through energy fractions of the subjets in reconstructing the W/Z-like particles in the diboson search. Angular correlations of X reconstructed jets can in turn be used to determine the spin of R once larger data points are available in the high invariant mass region. In the models where the BSM scalars (X and Y) are $SU(2)$ doublets, presence of light singly charged Higgs put constraints on them.

4. Associated resonance production

We have also addressed the question of resonance production. It could be produced through either gluon-initiated or quark-initiated process.

- Gluon-initiated process: Resonance interacts with the gluons through five- or six-dimensional operators. The R production through gluon fusion dictates that R should belong to $1, 8, 10, \overline{10}$ or 27-dimensional representations of $SU(3)$. It cannot be gauge boson because single production of massive gauge boson is forbidden by the Landau–Yang theorem. In the case of scalar R, all the coloured representations are allowed as far as its production is concerned but the required final state from R decay allows only colour singlet scalar, which could interact with the gluons through the following effective interactions
  - $G^{\mu\nu}\, G_{\mu\nu}\, R$
  - $G^{\mu\nu}\, G_{\mu\nu}\, R^{\dagger}\, R$.

  The tree-level corrections to the ρ parameter limit R choices to $1(1,\ 1,\ 0), 2(1,\ 2,\ \pm\frac{1}{2})$ or $7(1,\ 7,\ \pm 2)$-dimensional representations of $SU(2) \times U(1)$ [18].
- Quark-initiated process: If R is a gauge boson, then SM gauge group has to be extended. In different ultraviolet models, quarks could have different interactions with the gauge bosons but for the massive 2 TeV gauge bosons, one could have typical signatures as W' or Z' models. In the case of scalar R, it can have renormalizable as well as higher-dimensional interactions with quarks. The possible representations of R are listed in [14].

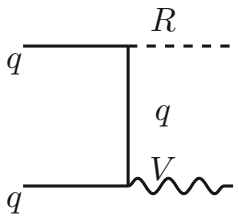

Figure 3. Feynman diagram for the quark-initiated RV production process.

Another interesting possibility is that it could also be produced in association with vector bosons. Quarks have tree-level coupling with the electroweak gauge bosons. In quark-initiated process, we could have $W/Z/\gamma$ emitted with the resonance. Gluons could have self-couplings in addition to the tree-level couplings with the quarks (see the Feynman diagrams in figures 3 and 4). Gluon can be emitted with the resonance from the initial quark or gluon leg. Therefore, associated production of R with gluon does not provide any information about the initial state. However, the associated production of R with $W/Z/\gamma$ will ensure that the resonance is produced through quark-initiated process. The schematic form of this process is

$$qq \to RV \to WW + W/Z/\gamma \to JJ + l\nu/ll/\gamma. \quad (1)$$

Clearly, associated RV production is an important channel to be considered at 13 TeV. One can look for $JJl\nu$ and $JJl^{+}l^{-}$ final states for RW and RZ search respectively. In order to estimate this cross-section, one has to specify the model. We consider spin-0 resonance produced through quark-initiated process. We assume

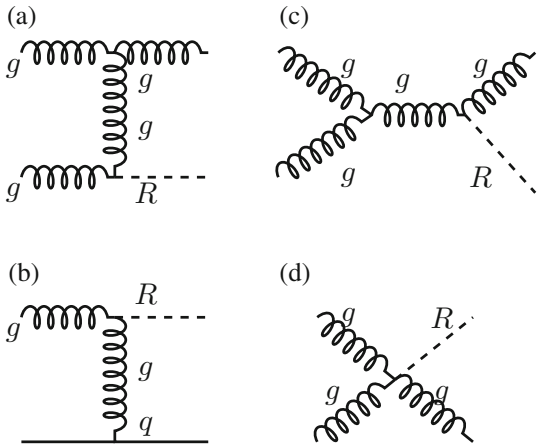

Figure 4. Feynman diagrams for the associated production of R with jets.

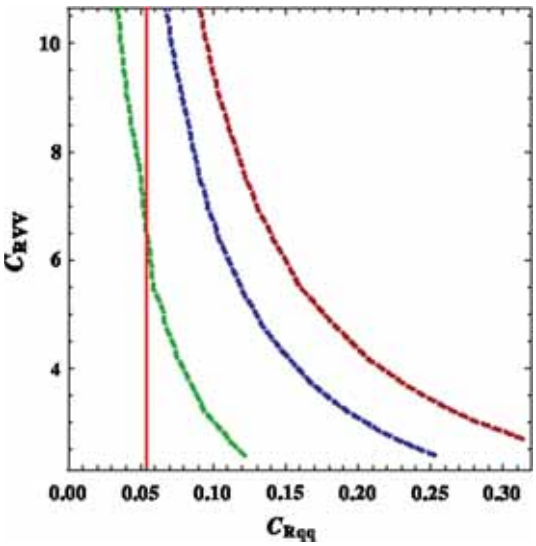

Figure 5. Contours of constant $\sigma(pp \to R \to WW)$ (fb) in C_{Rqq}–C_{RVV} plane. The maroon, blue and green dotted curves denote 10 fb, 5 fb and 1 fb cross-section contours respectively. The red solid line is the projected dijet bound at 14 TeV.

R is a scalar having Higgs-like couplings and it couples only to light quarks and massive gauge bosons at tree level. Diboson final states, $pp \to R \to VV$, involve two couplings C_{Rqq} (production) and C_{RVV} (decay). The C_{Rqq} coupling also determines dijet cross-section. In figure 5, we present the parameter space consistent with both dijet and diboson bounds. The dijet bound requires $C_{Rqq} < 0.33$. The parameter space below the maroon curve is allowed by diboson search. The straight line parallel to the y-axis is the projected 14 TeV dijet bound. In the allowed parameter space, the width of R is less than 10% of its mass.

For the two benchmark values, chosen from the allowed parameter space, we calculate the cross-section

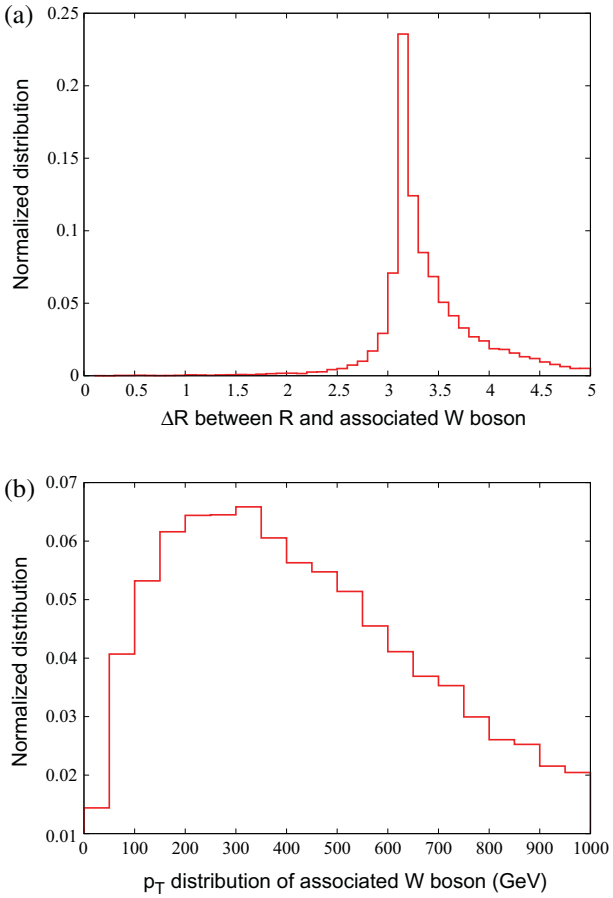

Figure 6. (**a**) Distribution of ΔR between R and W and (**b**) p_T distribution of W produced in association with R.

for RW and RZ processes. The main backgrounds for these processes are W/Z+jets. To verify that the lepton coming from the decay of gauge boson is well separated, we plot the ΔR distribution between W and R, and p_T distribution of W-boson in figure 6. From these figures one can see that the lepton is well separated and carries enough p_T that it is possible to see this signature. The expected number of events for $JJl\nu$ and JJl^+J^- channels are shown in table 2. Here, we demand the JJ pair invariant mass to be in the 1.8–2.2 TeV range. In the case of $JJl\nu$, we put p_T^l and $\not{E}_T$ cut, $30 < p_T^l, \not{E}_T < 350$ GeV, and use the same p_T^l cut for $JJll$ final state. There is another way to ensure the production mechanism of R. When R is produced via a quark-initiated process, the total charge of the final-state leptons integrated over all the events is positive. However, in the case of gluon-initiated process, this number would be 0.

One could also get three gauge bosons from the diagram shown in figure 7. This process will also have the same signature as the associated production (RW and RZ). But these can be distinguished from various

Table 2. Expected number of events for the $JJl\nu$ and $JJll$ channels from RW and RZ associated production for couplings $C_{Rqq} = 0.3$ and $C_{RVV} = 2.67$.

$\sqrt{s}$	8 TeV	13 TeV
Total number of generated events	20000	20000
$\sigma(pp \to RW)$	5 fb	75.6 fb
$JJl\nu$	277	161
$\sigma(pp \to RZ)$	2.2 fb	32.0 fb
$JJll$	101	69

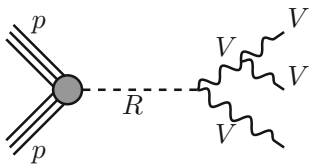

Figure 7. Feynman diagram for three-vector bosons final state.

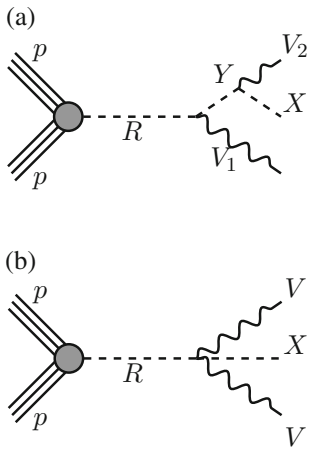

Figure 8. Feynman diagram for (**a**) the resonance decaying to two vector bosons and a BSM particle and (**b**) three-body resonance decay having two vector bosons and one BSM particle in the final state.

kinematic distributions. For example, gauge bosons will be highly energetic as they are coming from the 2 TeV resonance which will not be true for the gauge boson emitted from quark leg.

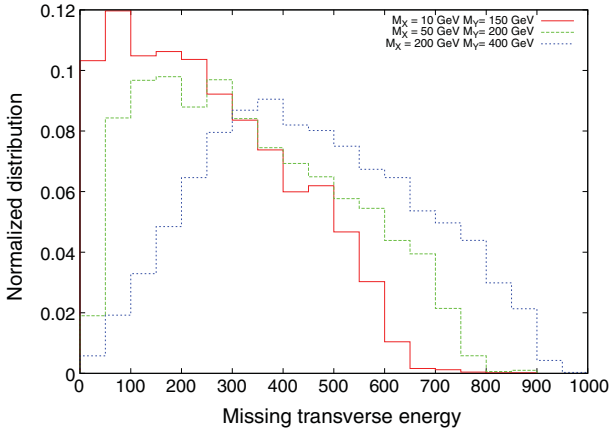

Figure 9. $\not{E}_T$ distribution when X decays invisibly for three different sets of X and Y masses as shown in the inset.

5. Three-particle final state

It has been argued in ref. [19] that the resonance can also decay to three particles in the final state as shown in figure 8a ($pp \to V_1 V_2 X$). By generating the parton level events for this process, we explore the possibility of this final state mimicking diboson final state. In this case, we have two BSM particles (X and Y) in addition to the resonance. The BSM particle X can decay visibly or invisibly. It cannot decay to leptonic final states because no excess has been reported for semileptonic/leptonic channels. If X decays invisibly, there will be p_T asymmetry between the visible final-state particles.

In table 3, we present the fraction of events which could pass the p_T asymmetry cut for different benchmark values of X and Y masses. We can see that only 29% of the events pass this cut, that too only when X is very light. In figure 9, we present the $\not{E}_T$ distribution at 13 TeV. One can confirm this decay by looking at two fat jets and $\not{E}_T$ signal.

The second possibility is that when X decays to hadronic final states. Then we look for the fraction of events which fall within the fat jet radius (figure 10 and table 4). Although 86% of the events (for heavy M_X) have X decay products within the fat jet radius but in

Table 3. Fraction of events passing different p_T^A asymmetry cuts $(p_T^{V_1} - p_T^{V_2})/(p_T^{V_1} + p_T^{V_2})$, $1.8 < m_{V_1V_2} < 2.2$ TeV and X decays invisibly.

M_Y (GeV)	M_X (GeV)	$p_T^A < 0.15$	$p_T^A < 0.25$	$p_T^A < 0.5$
150.0	10.0	0.29	0.29	0.29
200.0	50.0	0.15	0.15	0.15
300.0	50.0	0.15	0.16	0.16
300.0	100.0	0.062	0.064	0.064
400.0	200.0	0.00	0.00	0.00

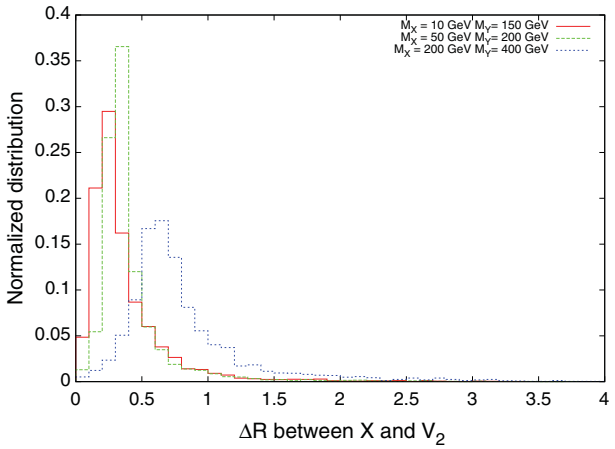

Figure 10. ΔR distribution between X and V_2 for three different sets of X and Y masses as shown in the inset.

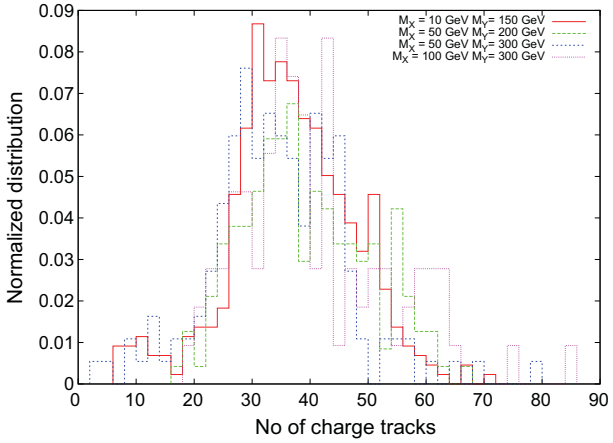

Figure 11. Normalized charge multiplicity distribution for the highest p_T jet for three benchmark points.

Table 4. Fraction of events having X decay products within fat jet radius, for different values of Y and X mass.

M_Y (GeV)	M_X (GeV)	Fraction of the events with $\Delta R < 1.2$
150.0	10.0	0.97
200.0	50.0	0.97
300.0	50.0	0.86
300.0	100.0	0.91
400.0	200.0	0.86

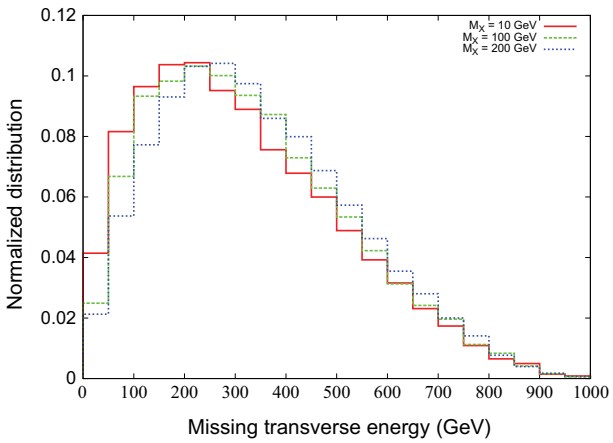

Figure 12. Distribution of $\not{E}_T$ when X decays invisibly for three different sets of X mass as shown in the inset.

Table 5. Fraction of events passing p_T asymmetry ($p_T^A = (p_T^{V_1} - p_T^{V_2})/(p_T^{V_1} + p_T^{V_2})$) and invariant mass ($1.8 < m_{V_1V_2} < 2.2$ TeV) cut when X decays invisibly for the diagram shown in figure 8b.

M_X (GeV)	Fraction of events with $p_T^A < 0.15$
10.0	0.16
50.0	0.14
80.0	0.11
100.0	0.10
120.0	0.08
150.0	0.05
200.0	0.02

this case jet mass of one of the fat jet will peak around M_Y instead of gauge boson. Jet substructure will be different and one has to look for two parents instead of one. In figure 11, we present the normalized distribution of the number of charge tracks inside the fat jet.

Another possible three-particle final state could arise from the four-point vertex (figure 8b). We also explore the possibility of this final state mimicking diboson excess. Again we look for the fraction of events passing p_T asymmetry cut for invisible X decay and plot the $\not{E}_T$ distribution of X in figure 12 (table 5). We can see that at most 16% of the events can pass this cut, that too when X is very light. In the case of visible decay, for a few benchmark points, in table 6, we show the fraction of events where X falls within the radius of the fat jet of one of the gauge bosons.

In these topologies, the final state is such that two of the particles mimic the signal obtained from the W/Z bosons and the third particle is not detected with the ATLAS diboson analysis cuts. The reason behind this can be two-fold. First, the third particle can decay into invisible final states and hence will not be detected. But in this case the p_T asymmetry and the invariant mass cut will be able to discard most of these events. This requires the mass of the third hidden particle to be $\lesssim$100 GeV. Otherwise, large loss in invariant mass or p_T asymmetry would not pass the experimental cuts. Secondly, even if the third particle decays to visible final states, there is a possibility that the third particle is within the fat jet

Table 6. Fraction of events having X decay products within fat jet radius for different values of X mass.

M_X (GeV)	Fraction of the events with $\Delta R < 1.2$
10.0	29.0
50.0	27.0
80.0	28.7
100.0	27.8
120.0	27.3
150.0	27.4
200.0	26.4

formed by one of the gauge bosons and the decay products of both of them will be seen as a single fat jet. This process is more favourable for light third particle. When R, X and Y are either singlets or doublets, in addition to the $2 \to 2$ process, the $2 \to 3$ process can also, in certain kinematic regimes, provide a signal to the diboson channel. Here we point out that all the models which attempt to explain the diboson excess with a three-body final state suffer from a set of common constraints. With more number of massive particles in the final state, the phase space suppresses the cross-section. The kinematic cuts which ensure that the two fat jets in the final state have a small relative p_T and large separation also add further suppression in this topology. The couplings need to be very large to get a large enough total cross-section after the cuts, so that the required diboson excess is satisfied.

6. Conclusion

We have analysed the phenomenological signatures of the BSM resonance to identify its nature and provide probable signatures for LHC 13 TeV searches.

Gauge bosons can decay to leptonic channels also, where no excess has been reported. We estimate the expected number of events in semileptonic and leptonic processes. We have suggested different BSM particle final states from the resonance decay which can mimic diboson excess and explain the absence of excess in semileptonic processes. We have addressed the question of whether the resonance production is a quark-initiated or a gluon-initiated process by looking at the associated production of the resonance with gauge boson. We provide a catalogue of possible final-state BSM particles (decay products of the resonance) as well as methods to distinguish them by looking at the jet substructure, the number of charged tracks inside the jet, $\not{E}_T$ distribution etc.

Acknowledgements

This talk is based on the work done in collaboration with B Bhattacherjee, P Byakti, J Lahiri and G Mendiratta.

References

[1] ATLAS Collaboration: G Aad *et al*, arXiv:1506.00962 [hep-ex]
[2] ATLAS Collaboration, ATLAS-CONF-2016-055
[3] J Hisano, N Nagata and Y Omura, *Phys. Rev. D* **92**, 055001 (2015), arXiv:1506.03931 [hep-ph]
K Cheung, W Y Keung, P Y Tseng and T C Yuan, *Phys. Lett. B* **751**, 188 (2015), arXiv:1506.06064 [hep-ph]
B A Dobrescu and Z Liu, *Phys. Rev. Lett.* **115**, 211802 (2015), arXiv:1506.06736 [hep-ph]
A Alves, A Berlin, S Profumo and F S Queiroz, *J. High Energy Phys.* **1510**, 076 (2015), arXiv:1506.06767 [hep-ph]
Y Gao, T Ghosh, K Sinha and J H Yu, *Phys. Rev. D* **92**, 055030 (2015), arXiv:1506.07511 [hep-ph]
Q H Cao, B Yan and D M Zhang, *Phys. Rev. D* **92**, 095025 (2015), arXiv:1507.00268 [hep-ph]
J Brehmer, J Hewett, J Kopp, T Rizzo and J Tattersall, *J. High Energy Phys.* **1510**, 182 (2015), arXiv:1507.00013 [hep-ph]
[4] B A Dobrescu and Z Liu, *J. High Energy Phys.* **1510**, 118 (2015), arXiv:1507.01923 [hep-ph]
J Heeck and S Patra, *Phys. Rev. Lett.* **115**, 121804 (2015), arXiv:1507.01584 [hep-ph]
B C Allanach, B Gripaios and D Sutherland, *Phys. Rev. D* **92**, 055003 (2015), arXiv:1507.01638 [hep-ph]; *J. High Energy Phys.* **1602**, 084 (2016), arXiv:1507.01681 [hep-ph]
G Cacciapaglia and M T Frandsen, *Phys. Rev. D* **92**, 055035 (2015), arXiv:1507.00900 [hep-ph]
T Abe, R Nagai, S Okawa and M Tanabashi, *Phys. Rev. D* **92(5)**, 055016 (2015), arXiv:1507.01185 [hep-ph]
M E Krauss and W Porod, *Phys. Rev. D* **92**, 055019 (2015), arXiv:1507.04349 [hep-ph]
P S Bhupal Dev and R N Mohapatra, *Phys. Rev. Lett.* **115**, 181803 (2015), arXiv:1508.02277 [hep-ph]
S F Ge, M Lindner and S Patra, *J. High Energy Phys.* **1510**, 077 (2015), arXiv:1508.07286 [hep-ph]
F F Deppisch, L Graf, S Kulkarni, S Patra, W Rodejohann, N Sahu and U Sarkar, *Phys. Rev. D* **93**, 013011 (2016), arXiv:1508.05940 [hep-ph]
[5] U Aydemir, D Minic, C Sun and T Takeuchi, *Int. J. Mod. Phys. A* **31**, 1550223 (2016), arXiv:1509.01606 [hep-ph]
P Coloma, B A Dobrescu and J Lopez-Pavon, *Phys. Rev. D* **92**, 115023 (2015), arXiv:1508.04129 [hep-ph]
T Bandyopadhyay, B Brahmachari and A Raychaudhuri, *J. High Energy Phys.* **1602**, 023 (2016), arXiv:1509.03232 [hep-ph]
R L Awasthi, P S B Dev and M Mitra, *Phys. Rev. D* **93**, 011701 (2016), arXiv:1509.05387 [hep-ph]

P Ko and T Nomura, *Phys. Lett. B* **753**, 612 (2016), arXiv:1510.07872 [hep-ph]
J H Collins and W H Ng, *J. High Energy Phys.* **1601**, 159 (2016), arXiv:1510.08083 [hep-ph]
B A Dobrescu and P J Fox, *J. High Energy Phys.* **1605**, 047 (2016), arXiv:1511.02148 [hep-ph]

[6] L Bian, D Liu and J Shu, arXiv:1507.06018 [hep-ph]
K Lane and L Pritchett, *Phys. Lett. B* **753**, 211 (2016), arXiv:1507.07102 [hep-ph]
M Low, A Tesi and L T Wang, *Phys. Rev. D* **92**, 085019 (2015), arXiv:1507.07557 [hep-ph]
A Carmona, A Delgado, M Quirs and J Santiago, *J. High Energy Phys.* **1509**, 186 (2015), arXiv:1507.01914 [hep-ph]
C W Chiang, H Fukuda, K Harigaya, M Ibe and T T Yanagida, *J. High Energy Phys.* **1511**, 015 (2015), arXiv:1507.02483 [hep-ph]
V Sanz, *Adv. High Energy Phys*. **2016**, 3279568 (2016) arXiv:1507.03553 [hep-ph]
C Niehoff, P Stangl and D M Straub, *J. High Energy Phys.* **1601**, 119 (2016), arXiv:1508.00569 [hep-ph]
H S Fukano, S Matsuzaki, K Terashi and K Yamawaki, *Nucl. Phys. B* **904**, 400 (2016), arXiv:1510.08184 [hep-ph]

[7] Y Omura, K Tobe and K Tsumura, *Phys. Rev. D* **92**, 055015 (2015), arXiv:1507.05028 [hep-ph]
D Aristizabal Sierra, J Herrero-Garcia, D Restrepo and A Vicente, *Phys. Rev. D* **93**, 015012 (2016), arXiv:1510.03437 [hep-ph]
J Brehmer,A Freitas, D Lopez-Val and T Plehn, *Phys. Rev. D* **93**, 075014 (2016), arXiv:1510.03443 [hep-ph]
S Jung, Y W Yoon and J Song, *Phys. Rev. D* **93**, 055035 (2016), arXiv:1510.03450 [hep-ph]
Y Kikuta and Y Yamamoto, *Eur. Phys. J. C* **76**, 297 (2016), arXiv:1510.05540 [hep-ph]
C H Chen and T Nomura, *Phys. Rev. D* **92**, 115021(2015), arXiv:1509.02039 [hep-ph]
S Zheng, arXiv:1508.06014 [hep-ph]

[8] W Chao, *Phys. Lett. B* **753**, 117 (2016), arXiv:1507.05310 [hep-ph]

[9] C H Chen and T Nomura, *Phys. Lett. B* **749**, 464 (2015), arXiv:1507.04431 [hep-ph]

[10] C Petersson and R Torre, *J. High Energy Phys.* **1601**, 099 (2016), arXiv:1508.05632 [hep-ph]

[11] B C Allanach, P S B Dev and K Sakurai, *Phys. Rev. D* **93**, 035010 (2016), arXiv:1511.01483 [hep-ph]

[12] H M Lee, D Kim, K Kong and S C Park, *J. High Energy Phys.* **1511**, 150 (2015), arXiv:1507.06312 [hep-ph]
S Fichet and G von Gersdorff, *J. High Energy Phys.* **1512**, 089 (2015), arXiv:1508.04814 [hep-ph]

[13] ATLAS Collaboration, ATLAS-CONF-2015-045

[14] B Bhattacherjee, P Byakti, C K Khosa, J Lahiri and G Mendiratta, *Phys. Rev. D* **93**, 075015 (2016), arXiv:1511.02797 [hep-ph]

[15] A Belyaev, N D Christensen and A Pukhov, *Comput. Phys. Commun.* **184**, 1729 (2013), arXiv:1207.6082 [hep-ph]

[16] T Sjostrand, S Mrenna and P Z Skands, *J. High Energy Phys.* **0605**, 026 (2006), hep-ph/0603175

[17] M Cacciari, G P Salam and G Soyez, *Eur. Phys. J. C* **72**, 1896 (2012), arXiv:1111.6097 [hep-ph]

[18] G Bhattacharyya, *Rept. Prog. Phys.* **74**, 026201 (2011), arXiv:0910.5095 [hep-ph]

[19] J A Aguilar-Saavedra, *J. High Energy Phys.* **1510**, 099 (2015), arXiv:1506.06739 [hep-ph]